IEEE Access
Multidisciplinary | Rapid Review | Open Access Journal

SPECIAL SECTION ON CHALLENGES AND ENDEAVORS OF RADIATED RADIO FREQUENCY TESTS FOR 5G RADIOS

Received October 30, 2020, accepted November 8, 2020, date of publication November 17, 2020, date of current version December 7, 2020.

*Digital Object Identifier 10.1109/ACCESS.2020.3038597*

# Multiple CATR Reflector System for Multiple Angles of Arrival Measurements of 5G Millimeter Wave Devices

**CORBETT ROWELL, (Senior Member, IEEE), BENOIT DERAT, AND ADRIÁN CARDALDA-GARCÍA**

Rohde & Schwarz GmbH, 81671 Munich, Germany

Corresponding author: Corbett Rowell (corbett.rowell@rohde-schwarz.com)

**ABSTRACT** This paper presents a novel method using multiple compact antenna test range (CATR) reflectors to perform simultaneous multiple angle measurements for 5G devices that are capable of beam-forming in the millimeter wave frequency range. Four CATR reflectors and their respective feed antennas are arranged on a planar semi-circle arc with the device under test placed on a positioner at the center of the arc. This arrangement is designed to generate four planar wavefronts with different incidences, realizing up to five pairs of angular spreads or four switched/simultaneous angles of arrival. The objective of this setup is to reproduce configurations involving multiple base-stations radiating from different directions. The initial target application is radio resource management (RRM) testing, where the execution of mobility procedures and radio link monitoring of a 5G millimeter wave device are evaluated. The reflectors create far-field conditions at the device under test for quiet zones up to 30 cm in diameter inside a portable system with a footprint of 3.25 × 1.4 meters. The applicability of the approach to RRM testing is demonstrated through measurements, performed with both sinusoidal and modulated signals, using horn antennas and commercial 5G devices.

**INDEX TERMS** 5G mobile communication, antenna measurements, millimeter wave communications, MIMO, mobile radio mobility.

## I. INTRODUCTION

In 5G millimeter wave frequency bands (FR2), there are several measurement applications requiring multiple angles of arrival for device characterization: MIMO (a multiple-input multiple-output technique used in both 4G and 5G to increase data speeds) with two or more spatial layers, RF (radio frequency) fading with multiple impinging waves, simultaneous in-band and spurious emissions threshold monitoring, and Radio Resource Management (RRM) [1]. One common example of an RRM scenario is when the 5G wireless device monitors the power levels from different base-stations and performs a handover to another base-station when the signal from the first one goes below a given threshold. It is assumed that these base-stations are located in the far-field (FF) of the wireless device.

The FF as calculated by the Fraunhofer formula of $R_{FF} = 2D^2/\lambda$, where $D$ is the quiet zone (QZ) or device under test (DUT) size and $\lambda$ is the wavelength, is roughly 24 meters at 40 GHz for a typical wireless device with a maximum diagonal of 30 cm. Although millimeter wave antenna array modules have apertures of 1-2 cm, it is likely that several modules are placed at different locations inside the wireless device that can be activated simultaneously, therefore requiring a 'blackbox' approach where the minimum quiet zone is bounded by the maximum DUT size. Measurement techniques for RRM and RF Fading include cabled measurements for wireless communications systems at frequencies below 7 GHz and wireless over-the-air (OTA) in the far-field of the DUT at frequencies above 24 GHz. While cabled measurements are faster and less complex, they are not as representative of real-world conditions as wireless OTA measurements.

In order to simulate multiple angles of arrival (or base-stations) in the FF of the DUT, probes (transmitting antennas) are typically placed at a distance corresponding to a desired quiet zone size and/or minimum allowed measurement uncertainty [2]. This approach is called a Direct Far-Field, or DFF,

The associate editor coordinating the review of this manuscript and approving it for publication was Wei Fan.

measurement method. For larger wireless devices in the millimeter wave region, this leads to very large measurement setups. If the probes are placed at distances much closer than the minimum Fraunhofer distance to the DUT, the measurement uncertainty increases. Using the example of a 30 cm quiet zone at 40 GHz, a DFF approach would require an RRM OTA system of at least 45 x 12 meters for an angular probe separation of 150°. An alternative is to use an indirect far-field (IFF) approach such as Compact Antenna Test Range (CATR) to reduce the range length, resulting in a decreased size of the measurement system.

This paper proposes a novel multiple CATR (multi-CATR) approach to reduce the required RRM measurement setup footprint (length x width) for a 30 cm quiet zone to 4.6 $m^2$, while maintaining low measurement uncertainty inside a defined quiet zone encompassing the entire wireless device [3]. This arrangement is made to simulate scenarios with multiple base-station pairs, from the DUT's point of view [4]. Several steps are carried out to demonstrate the relevance and accuracy of the solution, where the outcome of these tests are presented in this paper.

First, the proposed setup is modeled numerically with a commercial electromagnetic solver, in order to analyze possible scattering and diffraction points within the proposed system. Then, two multi-CATR prototypes are constructed: a benchtop system for a 20 cm QZ using a single axis positioner for 2D scans and a vertical system for a 30 cm QZ with a dual axis 3D positioner. Several measurements with complementary outcomes are performed by using a vector network analyzer (VNA) for radiation pattern measurements; multiple vector signal generators to generate 5G modulated signals while using a vector signal analyzer for demodulation; and a commercial 5G handset communicating in non-stand-alone (NSA) mode.

In Section II, the relevant background material for RRM specifications and CATR reflector design is presented. Section III analyzes the electromagnetic field distributions in simulations in order to design the two prototypes detailed in Section IV. Measurement results are discussed in Section V. Conclusions and perspectives towards future applications are finally delivered in Section VI.

## II. BACKGROUND

### A. RRM SPECIFICATIONS

For 5G FR2 RRM specifications, 3GPP (3rd Generation Partnership Project–a standards organization that develops protocols and specifies measurement methods for mobile communications) has defined five sets of base-station pairs, positioned at different relative angular separations [5]: 30°, 60°, 90°, 120°, and 150°. The wireless device performance is measured for each pair of Angles of Arrival (AoA) that are broadcasting on either different frequencies or in different time slots. Fig. 1 shows how the angular separations can be achieved with four antenna probe locations (as opposed to placing six antenna probes at

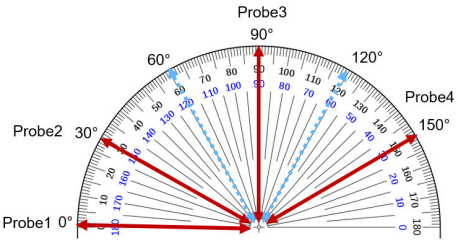


**FIGURE 1.** Realization of AoA separations for RRM.

0, 30, 60, 90, 120, 150°). Probes 2 and 3 are used for the angular spread of 60° and probes 2 and 4 are used for the angular spread of 120°. The probes are arranged in a single plane as only pairs of switched probes are considered in the 3GPP standards specifications. If the measurement setup includes a 2-axis positioner for the DUT, it can simulate a 3D multiple AoA system. By enabling and combining fast switching between the pairs of probes in the four probe system, individual probe power control, and positioner movements, it is possible to measure a dynamic AoA scenario simulating a moving DUT.

3GPP RRM test cases performed with such system include neighbor cell power measurements, mobility scenarios, beam management and radio link monitoring. The fundamental measurement parameter in RRM test cases is the Synchronization Signal-based Reference Signal Received Power (SS-RSRP) [1]. The SS-RSRP is defined as the linear average of the power contributions of the elements containing the synchronization signals. In all RRM test scenarios, the wireless device takes decisions based on the measured SS-RSRP for each of the cells.

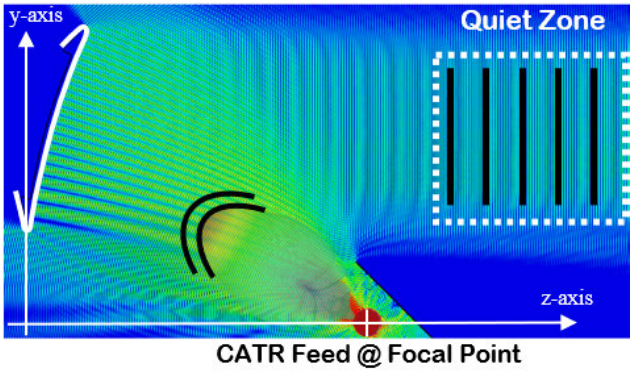


**FIGURE 2.** Typical offset CATR setup where the parabolic section is offset from its center at zero.

### B. CATR REFLECTOR DESIGN

A compact antenna test range (CATR) uses a paraboloid reflector with a feed antenna placed at its single focal point to transform a spherical wavefront into a planar wave distribution and vice versa (Fig. 2). In the test system presented in this paper, the reflectors use blended rolled edges to minimize diffraction and scattering inside the QZ and to optimize the size of the system [6].

Two CATR reflectors are developed for the two different measurement setups with two different quiet zone sizes of 20 cm and 30 cm with a respective reflector size of 42 × 43 cm and 52 × 54 cm. The lower paraboloid portion of the reflector is offset from the center by 20 cm in order to allow separation between the feed antenna that is placed at the focal point and the bottom of the rolled edges to prevent scattering of the reflected planar waves incident on the feed antenna into the quiet zone. The rolled edges of the reflectors are designed such that the minimum frequency limit of the reflector is 6 GHz. The upper frequency limit of 200GHz is determined by the measurement of the surface roughness variation of $R_q < 1$ micrometer and an arithmetic average surface roughness of $R_a < 1.6$ micrometers.

Both reflectors have a focal length of 70 cm in order to minimize the total system size. The short focal length for the larger quiet zone reflector is compensated by using a dual-polarized circular choke horn as a feed antenna with wide half-power beamwidth (HPBW) of 50-60 degrees. In addition to the wide HPBW, the circular choke horn has similar E-plane and H-plane patterns with side-lobe levels of -35 dB at 150° off boresight. The circular choke horn is fed by a waveguide orthomode transducer in order to support two orthogonal polarizations. As a final precaution, absorber blockers are added around each CATR feed antenna to minimize system scattering and DUT coupling.

Similar to a DFF system, an IFF CATR system can measure RF transceiver metrics instantaneously and directly in both Tx and Rx modes where measurement uncertainty is then generally dependent on the dynamic range of the measurement setup. The dynamic range of a CATR system can be much larger compared to the DFF approach. The improvement stems from the lower free-space path loss (FSPL) of CATR systems, which occurs only between the limited region where the spherical waves propagate between the feed and the reflector. RF cables inside an IFF system are also typically shorter than a DFF system, as the CATR feed antennas are often mounted close to the chamber walls or floor.

## III. NUMERICAL MODELING

This section starts with the description of the proposed multi-CATR system and results for electromagnetic simulations. These field visualizations are used to support the design of two experimental prototypes: (i) a smaller benchtop system with a quiet zone of 20cm and (ii) a larger vertical system with a quiet zone of 30cm; where Section IV discusses both experimental systems in more detail.

A CATR setup comprised of a dual-polarized feed antenna and a blended rolled edge paraboloid reflector is placed at each probe location marked in Fig. 1 at the angles of 0°, 30°, 90°, and 150°, forming a circular arc. The reflectors are arranged such that the collimated fields all cross in the center of the circular arc, where the DUT is placed for measurement. Electromagnetic simulations are then used to determine optimum locations for absorber blockers to prevent diffraction and scattering between adjacent CATR setups.

The simulations are carried out using a commercial physical-optics solver in CST Microwave Studio [7]. The physical optics numerical method allows the use of perfect absorbers to represent absorber blockers in a real system. There is still some diffraction in the simulation due to the boundary condition between the perfect absorber and air, but these components are filtered out using plane wave spectrum filtering post-processing.

For both benchtop and vertical CATR simulations, the feed antenna is first simulated using a time-domain code to generate complex far-field data in 1° step sizes at a frequency of 28 GHz. The data is then integrated as a field source into the physical optics solver. Electric field components are sampled throughout the entire simulation area for each feed excitation separately.

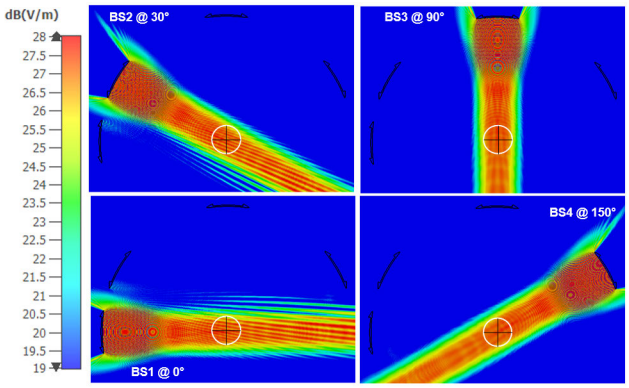


**FIGURE 3.** Electromagnetic field distributions for the multi-CATR benchtop system in a 20 cm QZ illustrating adjacent edge diffraction (top-view).

Fig. 3 shows the results of the simulations for each CATR reflector and the resulting fields inside the benchtop multi-CATR system. The location of the strongest scattering is between the reflectors placed at 0° and 30°, where the feed antennas scatter and diffract from the outer rolled edges of their neighboring reflectors. This scattering results in an additional 0.3 dB amplitude ripple across the 20 cm QZ.

Similar to the benchtop multi-CATR system simulation, each reflector in the vertical multi-CATR system generates a collimated beam at the desired angle (Fig. 4), but without the diffraction from adjacent reflectors in the benchtop simulation due to the absorber blockers placed between all of the reflectors. There is low back-scatter from the absorber blockers into the QZ due to the high FSPL of scattered millimeter waves.

## IV. MEASUREMENT SETUPS

Two measurement prototypes are constructed using different reflectors, different feed antennas, and different absorber layouts to characterize the general performance of the proposed multi-CATR reflector measurement system concept. The first prototype is constructed on a laboratory table using a basic setup in order to demonstrate proof of concept and to measure scattering locations required for absorber blocker placement

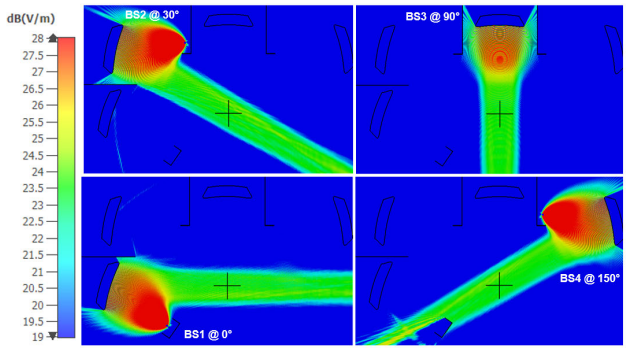


**FIGURE 4.** Electromagnetic field distributions for the vertical multi-CATR system with a 30 cm QZ using absorber blockers to suppress adjacent edge diffraction (side-views).

in the second prototype. The second prototype is designed to minimize the system footprint while increasing the quiet zone size by 50% and adding 3D positioning capability.

For both prototypes, the reflectors and feed antennas are individually aligned using lasers with the positioner in the center of the quiet zone as to reduce the measurement uncertainty (MU) of the feed and reflector misalignment. The quiet zone uniformity of the vertical CATR system is measured using two different methods: 2D field scanning of amplitude and phase from which the linear taper plus ripple can be extracted and the 3GPP method of quiet zone characterization.

The 3GPP method requires 322 separate 3D pattern measurements as a function of DUT angular and spatial placement where the limit is 0.6 dB for total radiated power (TRP) variation. The 3GPP quality of QZ MU metric then includes several uncertainty factors such as positioner influence, feed misalignment, chamber size, absorber thickness, and the influence of additional objects placed into the chamber such as a link antenna.

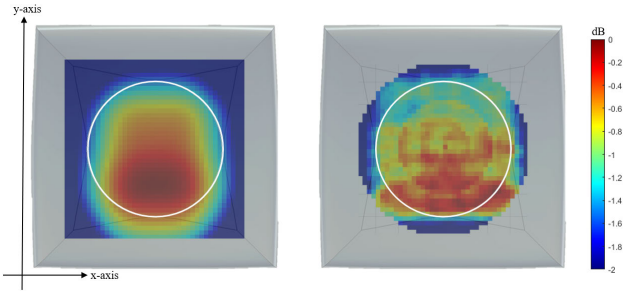


**FIGURE 5.** QZ 2D field scans for the reflector inside the vertical multi-CATR system: simulated (left-side) and measured (right-side) where the white circle shows QZ boundary at $R = 15$ cm from the center.

Fig. 5 compares the simulated QZ uniformity with the measured QZ at 28 GHz with a grid resolution of 1 cm for both scans. As is typical for offset parabolic CATR reflectors, the fields are higher in the lower portion of the reflector–this is due to the shorter distance between the focal point and the reflector surface, resulting in a lower FSPL compared to the top of the reflector. The difference in FSPL between the lower and upper potions (along the y-axis) of the reflector designed for the vertical multi-CATR system is 1 dB. Measurement values above this FSPL difference represent the scattering caused by the rolled edges and the other measurement uncertainties inside the CATR system.

The measured amplitude taper plus ripple extracted from the 2D scan in Fig. 5 is $A_x = 0.6 \pm 0.2$ dB in the symmetric portion of the reflector along the x-axis and $A_y = 1.1 \pm 0.2$ dB in the asymmetric portion of the reflector along the y-axis, whereas the phase tapers plus ripples are $P_x = 7 \pm 2°$ and $P_y = 8 \pm 2°$. The amplitude and phase taper measurements are similar to the simulation of the reflector QZ in an ideal environment of $A_{x,y} = [1.0, 0.8]$ dB and $P_{x,y} = [6, 8]°$ (ripple is near zero in the simulations). The 3GPP quality of QZ MU measurements are performed using a low-gain horn antenna (AINFO LB180400-10) as the DUT, resulting in an average quality of QZ MU of $0.3 - 0.4$ dB from 23.45 to 40.8 GHz and an average feed cross-polarization MU of less than 0.07 dB, as calculated according to 3GPP [8].

### A. MULTI-CATR BENCHTOP SYSTEM

Similar to the simulation setup, the four CATR setups are arranged on a large table at the specified probe angular locations (Fig. 6). Absorbers are placed in selected locations: between the feed antennas, behind the DUT to prevent rear-reflection from walls into the QZ, and between the 0° and 30° reflectors, as diffraction from the rolled edges can scatter into the feed. In this prototype, no absorber blockers are placed between the other reflectors at 30°, 90° and 150°. The dimensions of the setup are: $3.2 \times 2.2$ meters with a height of 0.8 meters above the table. The DUT is placed at the center of the circular arc formed by the four CATR setups on a fixture made of Rohacell (relative permittivity $\epsilon < 1.04$). The DUT and its Rohacell fixture are mounted on a single axis azimuth positioner in the plane containing all intended directions of the planar waves. The feed antennas are dual-polarized Vivaldi-type antennas with wide operational frequency bandwidth from 18 to 50 GHz. The FSPL of the benchtop system for each reflector at 40 GHz is 62.03 dB (using the distance from the feed antenna to the center of the reflector of 75.4 cm), resulting in an improvement of over 20 dB in dynamic range compared to the DFF approach for an equivalent QZ of 20 cm diameter (DFF has a range length of 10.6 meters and therefore a FSPL of 85 dB).

### B. MULTI-CATR VERTICAL SYSTEM

In the vertical multi-CATR system, four CATR setups are arranged inside a portable chamber with wheels along a vertical arc above the DUT mounted on a 3D positioner at the specified probe angular locations (Fig. 7). Absorber blockers are placed between all neighboring reflectors and below the reflector at 150° to prevent scattering from adjacent rolled edges into the quiet zone. The system footprint is $3.25 \times 1.4$ meters with a height of 2 meters. The FSPL at 40 GHz is almost the same as the benchtop system at

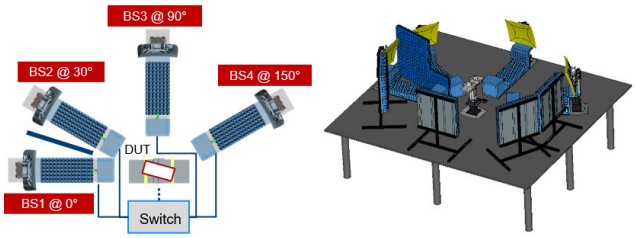


**FIGURE 6.** Benchtop multi-CATR system with four sets of CATR components arranged on a laboratory table.

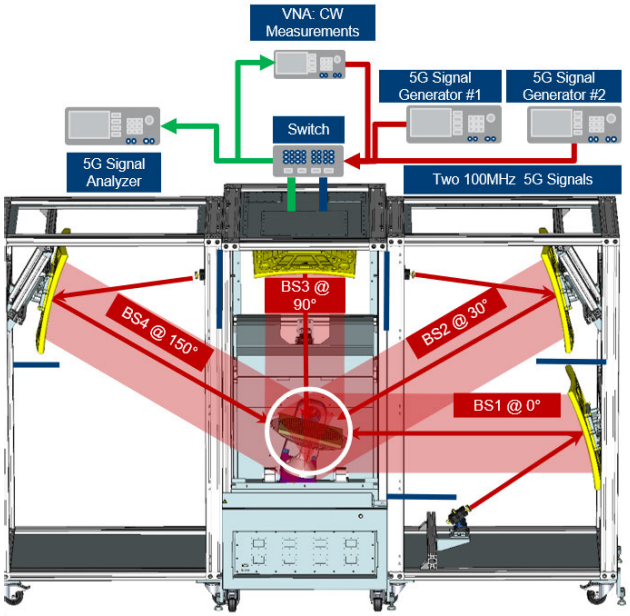


**FIGURE 7.** Vertical multi-CATR system with four sets of CATR components inside the shielded anechoic chamber.

62.15 dB, resulting in an improvement of almost 30 dB in dynamic range compared to the DFF approach for an equivalent QZ of 30 cm diameter (DFF has a range length of 24 meters and therefore a FSPL of 92 dB).

### C. MEASUREMENT INSTRUMENT SETUPS

Four dual-polarized CATR feed antennas containing eight cables are attached to an R&S$^{TM}$ OSP120 switching platform for both the benchtop and vertical multi-CATR prototypes with cable outputs routed to the appropriate measurement instrument. This allows the measurement instruments to connect to any single or pair of feed antenna polarizations inside the setup with a switching time of less than 10 ms.

Fig. 8 shows the generalized instrument switching setup for the three sets of measurements:

1) Non-Signaling with Continuous wave (CW): a four port R&S$^{TM}$ ZVA67 Vector Network Analyzer (VNA) is utilized for measurement of the S-parameters and antenna gain patterns. The goal of this measurement setup is to evaluate the influence of scattering from adjacent CATR systems on the DUT radiation performance.
2) Non-Signaling with modulated 5G waveforms: Whereas a CW measurement consists of measuring a single sinusoidal frequency of known power and phase, a modulated waveform measurement is a signal spread out across multiple frequencies. In this paper, the 5G waveform uses an orthogonal frequency-division multiplexing (OFDM) signal. Two R&S$^{TM}$ SMW200A vector signal generators (VSG) are used to generate 5G modulated signals spread out over a 100MHz bandwidth for each carrier from a pair of CATR setups simultaneously. A R&S$^{TM}$ FSW50 vector signal analyzer (VSA) measures the combined signals at the DUT, in the test scenarios of different impinging field directions and polarizations. No additional power amplifiers are used, so as to isolate the performance of the proposed CATR system from possible non-linear effects.
3) Signaling with active wireless device: a non-standalone (NSA) 5G wireless device is used to monitor signal levels between different pairs of base-stations at a single position. In non-standalone mode, the 5G wireless device uses a LTE base-station for signaling and control of the device. The LTE link antenna in the proposed multi-CATR systems is a single-polarized Vivaldi antenna R&S$^{TM}$ TS-F24V3 connected to a R&S$^{TM}$ CMW500 communication tester for LTE signaling. A R&S$^{TM}$ CMX500 5G radio communications tester sends and receives the 5G NR-FR2 base-station cell signal to the 5G wireless device.

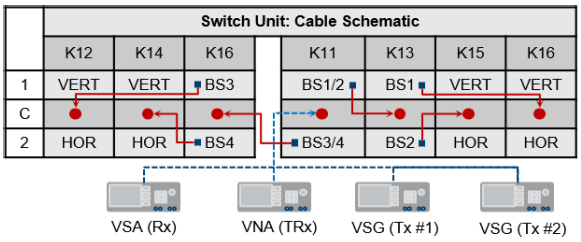


**FIGURE 8.** Instrument setup for proposed multi-CATR system.

The performance of the multi-CATR benchtop and vertical systems is measured using a horn antenna (AINFO LB180400-10), complying with radiation characteristics specified by 3GPP [8] that are similar to commercial 5G devices with an average gain of 10-13 dBi. In addition, a commercially available 5G handset with an unknown number of 5G FR2 antenna modules (black-box device) is used in the signaling test scenarios and connected in NSA mode to the base-station simulator (Fig. 9).

The non-signaling and signaling scenarios require different methods of system calibration prior to measurements inside the multi-CATR systems. For the CW non-signaling measurements, each CATR setup is separately calibrated using a calibration antenna located at center of the QZ. In the case of two

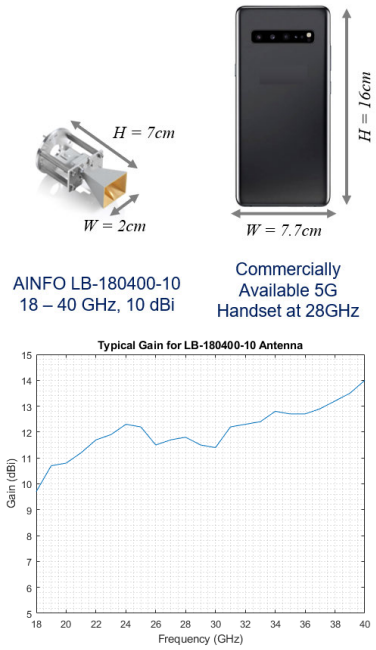


**FIGURE 9.** DUTs used for measurements & peak realized gain for LB-180400-10 antenna.

simultaneous 5G modulated signals, the power is adjusted on both of the signal generators until the power received by the horn DUT is equal for both channels at −62.3 dBm for all frequencies and both feed antenna polarizations (individually set for each frequency).

**TABLE 1.** Multiple reflector system measurements.

| Benchtop multi-CATR setup with 20 cm quiet zone | | | |
|---|---|---|---|
| DUT | Frequency | Distance from QZ Center | Scan Type and Signal |
| LB180400-10 | 28 & 40 GHz | R = 0 cm | 2D Scan CW only |
| 5G Handset | 27 - 28 GHz | R = 0 cm | 2D Scan Modulated 5G |
| **Vertical multi-CATR setup with 30 cm quiet zone** | | | |
| LB180400-10 | 24, 28, 32, 37, & 40 GHz | R = 0, 5, 10, 15 cm | 2D & 3D Scan CW & Mod. 5G |
| 5G Handset | 27 - 28 GHz | R = 0 cm | 2D Scan Modulated 5G |

Table 1 summarizes the measurements performed for both prototypes. For the non-signaling sets of measurements, the horn DUT is placed at different radii away from the center of the QZ in steps of 5 cm at $R = 0, 5, 10, 15$ cm in order to characterize QZ uniformity. There are two different scan types: (i) 2D Gain patterns with angular increments of 1° for both the E-plane and H-plane of the horn DUT and (ii) 3D Total Radiated Power (TRP) for a single AoA with angular increments $\Delta\phi$ and $\Delta\theta$ of 15°. The TRP is calculated using the discretized form of the Clenshaw-Curtis quadrature integral approximation [9], [10] where EiRP is defined as a singular value (or point) inside the 3D radiation pattern:

$$TRP = \frac{1}{2M}\sum_{i=1}^{N}\sum_{j=1}^{M}\left[EiRP_{\theta}(\theta_i,\phi_j) + EiRP_{\phi}(\theta_i,\phi_j)\right]W(\theta_i)$$

where the Clenshaw-Curtis weights are calculated iteratively using:

$$W(\theta_i) = \frac{c_i}{N}\left[1 - \sum_{j=1}^{int(N/2)}\frac{b_j}{4j^2-1}\cos(2j\theta_i)\right]$$

and

$$b_j = \begin{cases} 1, & \text{if } 2j = N \\ 2, & \text{otherwise} \end{cases} \quad \& \; c_i = \begin{cases} 1, & \text{if } i = 0 \text{ or } N \\ 2, & \text{otherwise} \end{cases}$$

The calculated total received power (TRxP) for the two modulated signals cannot be interpreted directly as the traditional TRP performance metric for two reasons: (i) the power received is the combined power from two signals that is set to be the same for all frequencies (regardless of peak realized gain variations) and (ii) due to the angular separation, elevation is measured over a full $2\pi$ instead of $\pi$. The TRxP metric is calculated using the Clenshaw-Curtis numerical integration method with a normalization factor of four times the single AoA received power. It is used for relative comparison of the 3D pattern results of simultaneous modulated signal measurements in order to derive the measurement uncertainty for blackbox DUT placed anywhere inside the 30 cm quiet zone.

## V. RESULTS AND DISCUSSION

### A. NON-SIGNALING WITH CW SIGNALS

In the interest of brevity, radiation pattern results are graphically presented for the H-Plane of the LB-180400-10 horn antenna for the frequency of 28GHz, whereas the measurement uncertainty (standard deviation of the results) are tabulated and presented in Fig. 11 to 13 for: (i) all relevant frequencies, (ii) both the peak realized gain and TRP, (iii) different reflector sizes, and (iv) different locations inside the QZ. The standard deviation of the results is a representation of the measurement uncertainty of the system for a blackbox DUT placed anywhere inside the quiet zone as it collects the measurement errors such as quiet zone size, cable reflections, feed antenna-DUT coupling, feed cross-polarization, reflector alignment, chamber size, and the measurement instruments.

The gain pattern results for each reflector angle are rotated by the expected angular difference, such that the boresight for each AoA is at $\theta = 0°$, hence providing easier pattern comparison. Fig. 10 shows the rotated radiation gain patterns for both the benchtop and vertical CATR systems, with the DUT positioned at a distance of $R = 0$ and $R = 15$ cm from the center of the QZ. Close agreement is observed, not only for different mirror angles, but also for different locations of the DUT inside the QZ. The similarities in the results between the two different test systems containing different reflectors/feed antennas/absorber layout demonstrate the wide applicability of the proposed multi-CATR concept.

There are differences in the gain pattern for the benchtop system below −10 dB. These differences occur from the feed antennas diffracting off the edges of the adjacent reflectors. Due to the different free space loss distances

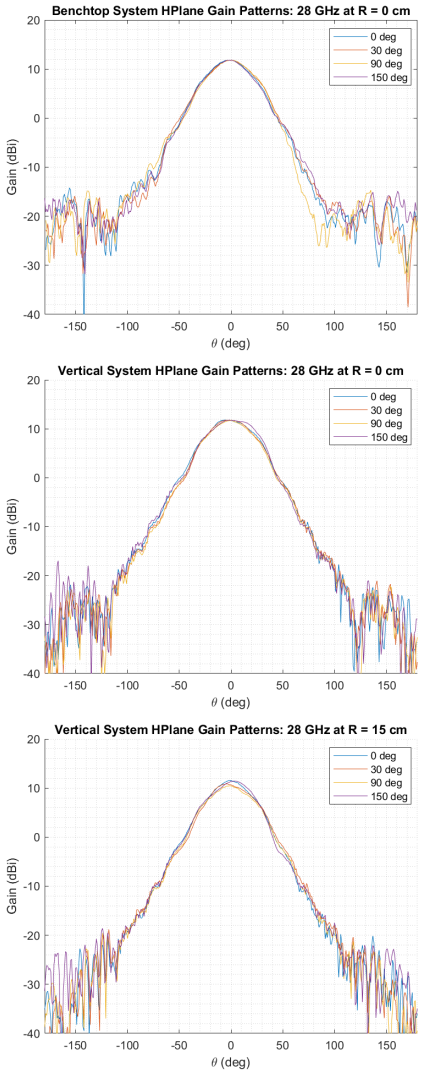


**FIGURE 10.** 2D Gain pattern measurement results at 28 GHz (CW signal) inside the benchtop multi-CATR system (top) and the vertical multi-CATR system (middle: $R = 0$ cm and bottom: $R = 15$ cm).

between the diffracted and the collimated CATR planar fields, this ripple in the gain pattern only appears 23-25 dB below the peak gain at angles greater than 50° from the boresight. By placing absorber blockers between all the reflectors in the vertical system, this gain pattern ripple is eliminated (as illustrated by the numerical modeling results in Figures 3 and 4).

Fig. 11 shows the peak realized gain and TRP mean values with standard deviations ($\sigma$) across the 30 cm QZ as a function of frequency. The measurement uncertainty for the peak realized gain measured at different locations inside the quiet zone for the vertical CATR system is below 0.6 dB for the entire 5G FR2 frequency band–this is expected as the cylindrical CATR quiet zone has a combined amplitude taper plus ripple of up to 1.3 dB between $R = 0$ to $R = 15$ cm. The measurement uncertainty for the 3D TRP measurements

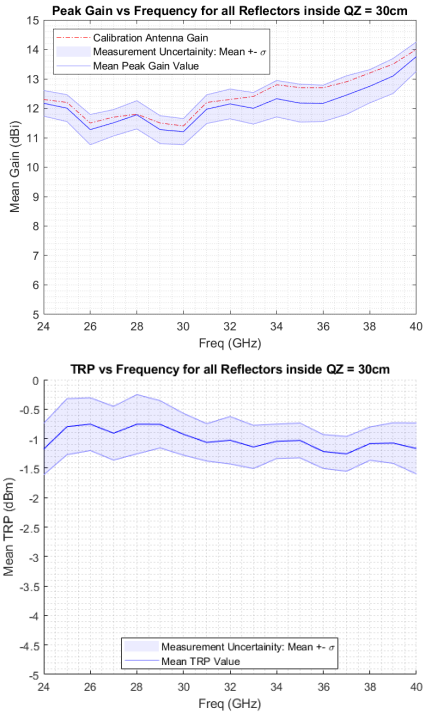


**FIGURE 11.** Measured mean and standard deviations for vertical CATR system with CW signals for $R = 0, 5, 10, 15$ cm, for peak gain (top) and TRP (bottom) as a function of frequency.

is between 0.3 to 0.5 dB across the measured frequency band from 24 to 40 GHz, corresponding to the 3GPP quality of QZ MU result presented in Section IV for a single reflector. The TRP measurement averages out the quiet zone amplitude errors over a spherical grid and therefore has a lower measurement uncertainty compared to a single point measurement such as peak realized gain.

### B. NON-SIGNALING WITH MODULATED 5G WAVEFORMS

In the modulated waveform measurements, it is demonstrated that the horn DUT is able to receive and distinguish between two simultaneous signals for different angular spreads in the vertical multi-CATR system. Two 5G signals are generated with OFDM modulation of 100 MHz signal bandwidth for the frequencies of 23.45, 28, 32, 37, and 40 GHz. The 5G modulated signals are transmitted through the CATR setups at different angles, but on the same feed polarization. The horn DUT is rotated such that an entire sphere is measured for both modulated signals arriving at two different angles. The signals are demodulated with the vector signal analyzer and the results presented as received power patterns. The horn DUT is placed at different distances from the center to characterize the influence of non-uniformities inside the QZ.

Fig. 12 shows the power pattern for different angular spreads. The low-gain horn is unable to distinguish between the planar waves coming from the reflectors placed at 0° and

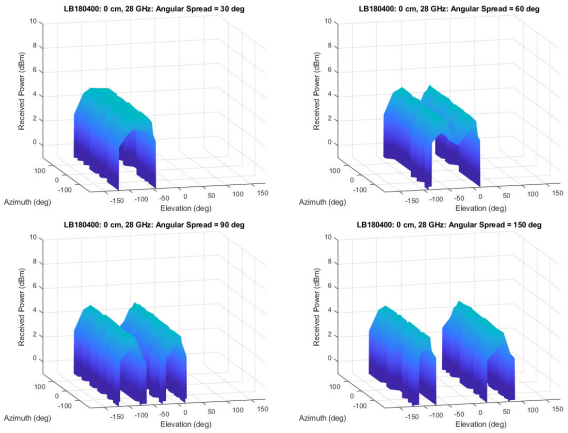


**FIGURE 12.** 5G modulated signal received power measurements for various angular spreads of 30, 60, 90 and 150° with low-gain horn at 28GHz.

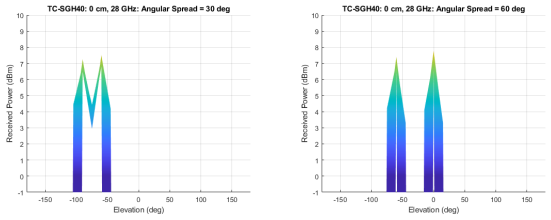


**FIGURE 13.** 5G modulated signal received power measurements at angular separations of 30° and 60° with a 20 dBi standard gain horn at 28GHz.

30° due to its large HPBW of 45° at 28 GHz. A 20 dBi standard gain horn (R&S$^{TM}$ TC-SGH40) with a HPBW of 20°, however, is able to separate out the different angles of arrival for the smallest angular spread of 30° as illustrated in Fig. 13.

The measurement uncertainty results for the peak gain and the TRxP of two simultaneous signals for the frequencies of 23.45, 28, 32, 37 and 40 GHz at different points within the QZ are presented in Fig. 14. The average peak gain standard deviation over frequency of 0.1 to 0.2 dB is much lower than for the measurement using CW. This is a result of the wideband signal which averages the received power errors over a 100 MHz bandwidth as the amplitude and phase ripple inside the CATR quiet zone is frequency dependent (diffraction from reflector edges and absorber blockers).

The TRxP standard deviation of $0.4 - 0.5$ dB in Fig. 11 is similar to the TRP CW measurement. This result could be further improved by increasing the dynamic range of the setup with additional power amplifiers and moving the measurement instruments closer to the CATR feed antennas. An active 5G device will have higher output power than the signal generator without additional cable losses, resulting in higher measurement dynamic. Both the peak realized gain and TRxP measurement uncertainties are within proposed 3GPP limits of 0.7 dB for 3D power measurements inside IFF systems for RRM.

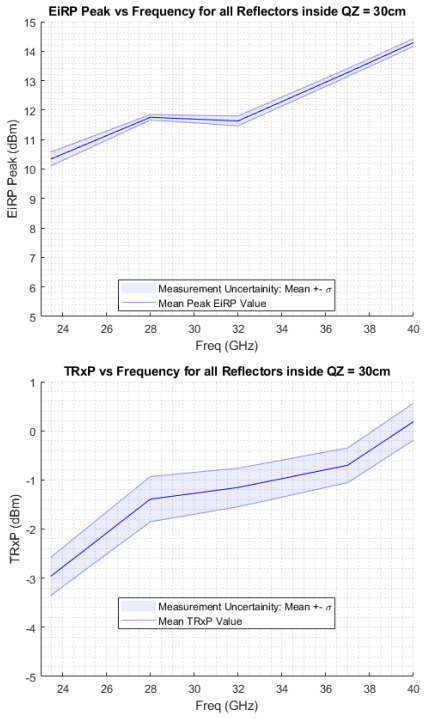


**FIGURE 14.** Measurement Uncertainty for Vertical CATR System with 5G modulated signals for $R = 0, 5, 10, 15$ cm. Top: Mean peak gain and Bottom: Mean TRxP.

### C. SIGNALING WITH ACTIVE WIRELESS DEVICE

The last set of measurements focuses on evaluating the accuracy of the SS-RSRP measurements in the proposed multi-CATR systems. A commercial wireless device supporting 5G NR FR2 is used for the tests, as depicted in Figure 9. The measurements are repeated 33 times for statistical significance, following the recommendations of 3GPP TS38.533 Annex G [5]. Three different scenarios are evaluated:

1) *One active cell: Comparison of different CATR systems*: the first set of measurements compares the SS-RSRP acquisition results in a single-CATR setup with those obtained in the benchtop and the vertical multi-CATR setups. In the multi-CATR setups, the mobile phone has been placed with its back facing the CATR at 90°.
2) *One active cell: Comparison of measurements in the center and the edge of the QZ*: the second set of measurements compares the results in the center of the QZ, $R = 0$ cm, with the results obtained at opposite QZ edges, $R = \pm 15$ cm.
3) *Two Active Cells*: Two active cells generate two AoAs at the wireless device. The Tx power level is changed by ±10dB every 20 iterations, in order to determine if the wireless device can accurately monitor both base-stations simultaneously. The CATR setups at 0 and 90° are used for this measurement scenario. The wireless device is placed such that its rear portion faces 45° (between the two CATR setups).

**TABLE 2. Test parameters for realized RRM measurement scenarios.**

| Parameter | Scenarios 1 and 2 | Scenario 3 |
|---|---|---|
| Method | SS-RSRP periodic reporting | |
| Iterations | 33 | 80 |
| NR-FR2 Cell 1 | n261 (27.55 GHz) | |
| NR-FR2 Cell 2 | - | n261 (27.925 GHz) |
| NR-FR2 Bandwidth | 100 MHz | |
| Expected SS-RSRP | -105 dBm / 120 kHz | See Fig. 17 |
| Angular Spread | - | 90° |

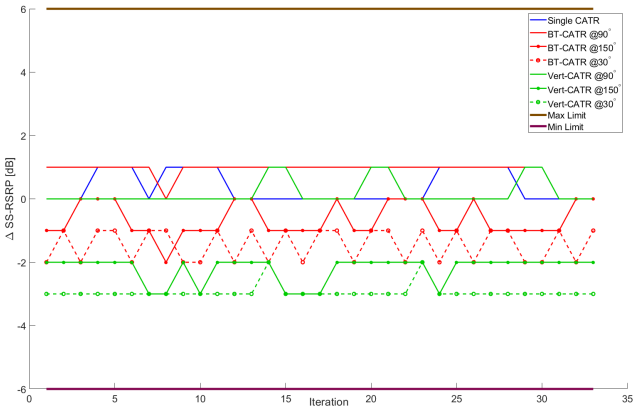


**FIGURE 15. RRM scenario #1: SS-RSRP reporting for one cell in multi-AoA setup.**

A LTE antenna attached to a base-station simulator, acting as the link antenna for NSA mode, is placed nearby the wireless device in the positioner as to maintain a stable link. The detailed configurations for all scenarios are described in Table 2.

Fig. 15 shows the difference between the expected SS-RSRP and the measured SS-RSRP for the first RRM test scenario. The results for the 90° reflector in both the benchtop and the vertical multi-CATR systems are similar to the single-CATR setup, demonstrating that the proposed multi-CATR arrangement has limited influence on the test results. The results for the other two CATR angles vary slightly, which is expected since the commercial 5G device's antenna gain is different at various incoming signal directions. The resulting SS-RSRP for all angles and both polarizations at different times, however, are well within the recommended RAN4 SS-RSRP maximum and minimum limits of ±6 dB of the expected SS-RSRP.

The results for the second RRM test scenario are shown in Fig. 16. It can be seen that the SS-RSRP measurement reports are within the recommended RAN4 SS-RSRP maximum and minimum limits of the expected SS-RSRP, both in the center and at the edges of the QZ ($R = \pm 15$ cm). The small variation of the measurements is a combination of multiple factors: (i) the variation of the amplitude of the 5G NR signal within the QZ–as demonstrated previously in Section V, this variation is less than 1dB (the 5G commercial wireless device has a SS-RSRP reporting

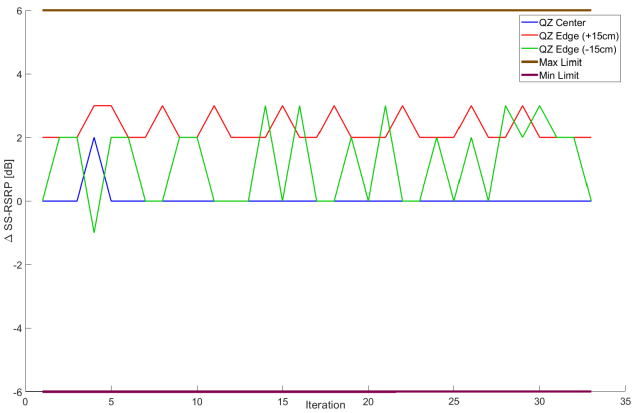


**FIGURE 16. RRM scenario #2: SS-RSRP reporting in the center ($R = 0$ cm) and at the edge of the QZ ($R = \pm 15$ cm).**

resolution of 1 dB); (ii) the wireless device placed at different distances from the center of the quiet zone, where the incoming signal direction varies from the wireless device's perspective, and consequently the antenna gain varies as well; and (iii) the wireless device's internal noise at low signal levels, as illustrated in Fig. 17. Similar to the first RRM test scenario, the 3GPP defined 5G commercial wireless device measurement accuracy is ±6 dB, [1], so this proposed multi-CATR system is well within the requirements.

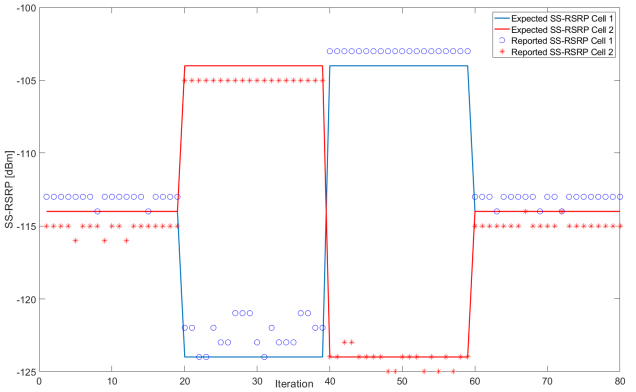


**FIGURE 17. RRM scenario #3: inter-frequency SS-RSRP reporting for 2 cells in multi-AoA setup.**

In the more realistic third RRM test scenario of two active base-station cells, it is seen that the wireless device is able to simultaneously receive signals from base-station cells located in multiple directions, even when one of them has significantly higher power than the other (Fig. 17). The measurements show that both cells are reporting within 1 dB of expected SS-RSRP for higher Tx Power (higher signal to noise ratio) and within $1 - 3$ dB of expected SS-RSRP for lower Tx Power (lower signal to noise ratio). Although the commercial wireless device has unknown specific gain values for different orientations and polarizations,

the expected values are based on the assumption that 3GPP requirements are met by the commercial wireless device.

As illustrated in Fig. 17, the switch between different Tx powers of 10 dB is correctly reported without any delays. The lowest expected SS-RSRP level (−124 dBm) is below the reference sensitivity limit defined by 3GPP and the internal noise of the commercial wireless device results in the higher measurement error for the lower Tx power. The reported SS-RSRP for Cell 1 is in general higher than for Cell 2, matching the results from the first RRM test scenario, where the SS-RSRP reports for the reflector at 30° are also higher than for the reflector at 150°. From these results, it can be deduced that the commercial wireless device has higher antenna gain when the signal is received from the top area of wireless device, consistent with the known antenna module placement.

## VI. CONCLUSION AND PERSPECTIVES

In summary, the proposed multi-CATR system is able to perform accurate measurements for different types of DUTs operating in either passive non-signaling or active signaling modes for both a single angle of arrival and multiple simultaneous angles of arrival. It is demonstrated that the proposed measurement system has low quiet zone measurement error with the different reflectors for different types of measurements using a variety of measurement instruments and signals. Due to the minimum disturbance of the adjacent reflectors, it is possible to perform combined RF and multiple angular measurements in a single measurement system.

As a consequence, this opens up a range of new applications for the multi-CATR system: (i) with separate transceivers for each reflector, spatial MIMO measurements can be performed; (ii) with additional displaced feeds from the focal point to shift the plane wave direction by up to $5 - 10°$, it is possible to construct RF Fading scenarios for 5G wireless device characterization; (iii) Intelligent reflecting surfaces (IRS), as proposed for 6G, can be measured by assigning a subset of reflector(s) as base-stations and the remaining subset as user devices, thereby performing a complete performance evaluation of the IRS for users and base-stations located in the far-field of each other; and (iv) placing antennas in other frequency bands at different reflector angles, allowing simultaneous wideband measurements from 6 to 140 GHz that are important for measurement of spurious out-of-band emissions together with in-band radiation performance.

## ACKNOWLEDGMENT

The authors would like to thank the following Rohde & Schwarz team members for assistance with conceptual discussions and measurements: Jose Fortes, Engelbert Tyroller, Anes Belkacem, and Mert Celik.

## REFERENCES

[1] *Requirements for Support of Radio Resource Management*, document V16.0.0 TS 38.133, TSG RAN; NR, 3GPP, 2019.
[2] *Verification of Radiated Multi-Antenna Reception Performance of User Equipment (UE)*, document TR 37.977, V14.5.0, 3GPP, 2017.
[3] C. Rowell, A. Cardalda-Garcia, and B. Derat, "CATR reflector measurement system with multiple reflectors for multiple angles of arrival in millimeter wave frequency bands," in *Proc. AMTA*. New York, NY, USA: Virtual, 2020, pp. 12–17.
[4] *On IFF Method for Multi-AoA Test Setup for RRM*, document RAN5 #85, R5-198221, Rohde & Schwarz, 2019.
[5] *UE Conformance Specification; Radio Resource Management (RRM)*, document TS 38.533, 3GPP, TSG RAN, NR, V16.1.0, 2019.
[6] W. Burnside, M. Gilreath, B. Kent, and G. Clerici, "Curved edge modification of compact range reflector," *IEEE Trans. Antennas Propag.*, vol. AP-35, no. 2, pp. 176–182, Feb. 1987.
[7] *CST Microwave Studio 2019 by Computer Simulation Technology*. Accessed: 2019. [Online]. Available: http://www.cst.com
[8] *User Equipment (UE) Conformance Specification; Radio Transmission and Reception; Part 2: Range 2 Standalone*, document TS 38.521-2, 3GPP; TSG RAN; NR, V16.5.0, Annex O.2.1, Oct. 2020.
[9] C. W. Clenshaw, A. R. Curtis, "A method for numerical integration on an automatic computer," *Numerische Mathematik*, vol. 2, pp. 197–205, Dec. 1966.
[10] P. J. Davis and P. Rabinowitz, *Methods of Numerical Integration*. San Diego, CA, USA: Academic, 1984.

**CORBETT ROWELL** (Senior Member, IEEE) was born in CA, USA, in 1972. He received the B.S. degree (Hons.) in physics from the University of California at Santa Cruz, in 1994, the M.Phil. degree in electrical and electronic engineering from The Hong Kong University of Science and Technology, in 1996, and the Ph.D. degree in electrical and electronic engineering from The University of Hong Kong, in 2013.

From 1996 to 2005, he worked extensively in the mobile antenna design industry, developing some of the first internal antennas for mobile phones working directly for antenna manufacturers and as the CEO of one of the first internal antenna design companies in Asia. He served as the Research and Development Director of the Hong Kong Applied Science and Technology Research Institute for almost a decade, where he focused on advanced RF systems. In 2013, he joined the China Mobile Research Institute as the Research and Development Director, where he is responsible for the development of massive MIMO base stations for 4.5G and 5G FR1. After China Mobile, he was a Professor of electrical engineering in Kazakhstan and an Adjunct Professor with The Hong Kong University of Science and Technology for two years. Since 2016, he has been a Senior Development Expert in over-the-air (OTA) and antenna measurement solutions with Rohde & Schwarz, Munich, Germany, where he has developed three new CATR systems and a new OTA extreme temperature testing method. He has written over 40 papers and holds almost 100 granted patents worldwide. His research interests include a wide breadth of wireless technologies from massive MIMO, antenna design, phased arrays, CATR-to-cloud RAN, fiber backhaul, and communications systems.

Dr. Rowell was a recipient of the 2018 Fred Ellersick Award for best original paper in the IEEE Communications Society for one of the first papers demonstrating hybrid beamforming in millimeter-wave base stations and the Inventor of the Year at Rohde & Schwarz in 2018.

**BENOIT DERAT** was born in Drancy, France, in 1979. He received the Engineering degree (Hons.) from Supélec, Gif-sur-Yvette, France, in 2002, and the Ph.D. degree (Hons.) in physics from University of Paris XI, Orsay, France, in 2006.

From 2002 to 2008, he worked with SAGEM Mobiles as an Antenna Design and Electromagnetics Research Engineer. During these years, he gained expertise in antenna measurements and simulations and actively contributed to innovation and international standardization in near-field techniques for human exposure assessment to radiofrequency waves. In 2009, he founded the company ART-Fi, which created the first vector-array SAR measurement system and initiated the IEC 62209-3 standard development. He operated as the CEO and the President of ART-Fi until 2017, before joining Rohde & Schwarz, Munich. He is currently leading the research and development for EMC, over the air (OTA), antenna, and A&D test systems as the Senior Director of Engineering. He is the author of more than 70 scientific conference and journal papers and an inventor on close to 30 patents relating to antenna and electromagnetic field measurements.

**ADRIÁN CARDALDA-GARCÍA** was born in Langreo, Asturias, Spain, in 1988. He received the M.S. degrees in telecommunication engineering and information technology and mobile network communications from the University of Oviedo, Spain, in 2012 and 2015, respectively.

From 2011 to 2012, he was a Student Research Assistant with the German Aerospace Center (DLR). Since 2012, he has been a Development Engineer and a 3GPP RAN5 Representative with Rohde & Schwarz, Munich. He is the author of one book, two articles, and almost ten inventions. In his role as a 3GPP Representative, he is involved in the definition of 5G NR specifications and is the Rapporteur of the 5G NR Positioning and RRM sub-work items in RAN5. His research interests include over-the-air testing methods for 5G FR2 and positioning technologies for cellular networks.

Mr. Cardalda-García was a recipient of the Scientific Award of the 2012 ITS World Congress in Vienna and three other awards for his master thesis.